ELSEVIER

Journal of Hydrology 272 (2003) 213–225

Journal of Hydrology

www.elsevier.com/locate/jhydrol

Spatial variability of the effective retardation factor in an unsaturated field soil

Mark J. Thomasson[a,*], Peter J. Wierenga[b,1]

[a]*Department of Hydrology, University of Arizona, Tucson, AZ, USA*
[b]*Department of Soil, Water, and Environmental Science, University of Arizona, Tucson, AZ, USA*

Abstract

A precisely controlled field study was conducted to determine flow and transport of water and bromide through an unsaturated soil. A 50 m × 50 m plot was instrumented with neutron probe access tubes, tensiometers, and solution samplers. Water containing bromide part of the time was applied at a steady flux of 1.85 cm d^{-1} for 24 days. The average degree of water saturation during water application was about 56%. The Hydrus 1-D model was used to optimize the saturated hydraulic conductivity parameter K_s, and the transport parameters D (dispersion coefficient) and R (used here as a 'bulk retardation coefficient'). The van Genuchten flow parameters θ_r, θ_s, α, and n were obtained from laboratory measurements on 11 cores taken 1.5 m below the soil surface along a transect through the plot. The estimated field K_s value increased with depth due to higher sand and gravel contents at depth. The mean dispersion coefficient for 13 locations at the 3 m depth was found to be 5.35 cm^2 d^{-1}, with a coefficient of variation of 52%. This resulted in a relatively small mean dispersivity value of 0.64 cm. The average R value was 0.63 with a range of 0.45–1.02 at 3 m (CV = 28%). The low R value is indicative of anion exclusion, immobile water, or some other phenomenon difficult to identify from field data. These field data indicate that if a transport model with a bulk retardation factor is used for predicting bromide transport through unsaturated soil a range of retardation values may need to be used. For our soil, the highest R value needed to be at least twice its lowest value.

Keywords: Transport factor; Spatial variability; Contaminant

1. Introduction

Prediction of contaminant transport through unsaturated field soils is strongly influenced by the soil hydraulic and chemical properties and processes. Variability in soil hydraulic properties can cause large spatial differences in rates of contaminant transport from the surface to the groundwater. This, and the fact that water and solutes are often unevenly applied over the soil surface both spatially and temporally, has caused solutes to arrive at depths at greatly varying times. Because the differences in arrival times are difficult to explain on the basis of the traditional convective transport equation, concepts such as immobile water, preferential flow or focused flow were introduced (van Genuchten and Wierenga, 1976; Beven and Germann, 1982; Roth et al., 1991). In addition, stochastic models (Dagan and Bresler, 1979; Russo and Bresler, 1981; Jury et al., 1982; Jury et al.,

* Corresponding author. Address. Department of Geography and Earth Science, University of North Carolina at Charlotte, 9201 University City Blvd., 450 McEniry, Charlotte, NC 28223–0001, USA.

E-mail addresses: mjthomas@email.uncc.edu (M.J. Thomasson), wierenga@ag.arizona.edu (P.J. Wierenga).

[1] Present address. Water Resources Research Center, 350 N., Campbell Avenue, Tucson, AZ 85721, USA. Tel.: +1-520-792-9591; fax: +1-520-792-8518.

0022-1694/03/$ - see front matter © 2002 Elsevier Science B.V. All rights reserved.
PII: S0022-1694(02)00266-4

1986; Russo, 1998) were developed and used to describe field data.

Soil chemical properties also affect transport of contaminants through vadose zone soils. In fact, in many cases these effects are of much greater importance than the hydraulic effects. Examples of chemical effects are equilibrium or time dependent sorption (Brusseau, 1994), ion exchange, and anion exclusion (Biggar and Nielsen, 1976; James and Rubin, 1986; Porro and Wierenga, 1993).

There now exist a variety of models (for a recent review see Simunek et al., 2003) that include many of the hydraulic and chemical processes that affect transport through the vadose zone. Unfortunately to use these models at a given field site one needs to know a large number of parameters that are used to describe the underlying physical and chemical processes. For example, Simunek et al., 2002 state that for a dual-permeability model, after some simplifications, still as a many as 10 parameters are needed. They continue by stating that little guidance is available as to how to obtain these parameters. Although comprehensive models, which are available, make it possible to gain an understanding of the influence of the various mechanisms and processes on the outcomes of these models, the lack of parameter values makes the use of these comprehensive models for real world situations impractical. For such situations, the use of simplified models is preferable. In this paper, we assume that the convective transport equation, in which chemical interactions are represented by a single effective retardation factor, can successfully be used to make field scale predictions of contaminant transport in the vadose zone. We test this hypothesis with results obtained from a precisely controlled field transport experiment.

2. Methods

2.1. Site description

The Maricopa Agricultural Center (MAC) located in Maricopa, AZ is situated within a northwest trending alluvial basin, situated within the Basin and Range region. The Basin and Range region is characterized by northwest to southeast trending mountain ranges separated by broad alluvial valleys (ADWR, 1993). The alluvium in the basin is anywhere from 60 to 150 m in thickness and is comprised primarily of unconsolidated to slightly consolidated sands and gravels. Some finer grained lenses are distributed throughout the unit. The regional groundwater table is at approximately 100 m depth. The site lies in the alluvium with a localized perched zone of groundwater at approximately 11–12 m depth. The region is in a semi-arid environment and receives approximately 20 cm of rainfall annually. Precipitation is characterized by intense, short duration summer storms and longer duration low intensity winter rains. The region experiences hot summers, and mild winters with an average annual temperature of 21 °C.

2.2. Description of tracer experiments

Solute transport tracer experiments were conducted on a 50 m × 50 m plot located within field plot F-115 at the MAC site (Fig. 1). The 50 m × 50 m

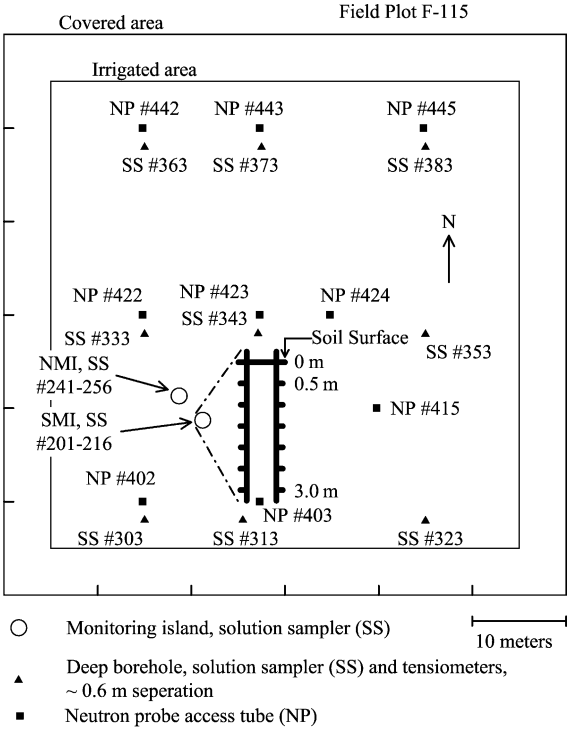

Fig. 1. Experimental plot F-115 at the MAC site showing locations where data was collected and monitoring island schematic.

plot was covered by a 60 m × 60 m, 0.081 cm thick Hypalon® pond liner to minimize surface evaporation. Two monitoring islands, shown as circles in Fig. 1, were constructed to access the subsurface using 3.5 m long by 1.53 m diameter corrugated steel, highway culverts placed vertically in 1.7 m diameter auger holes. The annular space between the soil and the corrugated steel culverts was backfilled using sieved native material. Through ports cut in the culvert walls, the undisturbed soil around each culvert could be accessed. Single-chamber solution samplers were installed through the walls of the north and south monitoring islands (NMI and SMI) on their east and west sides from 0.5 m to a depth of 3.0 m in 0.5 m intervals (Young et al., 1999a) using a rotary drill to make a slightly sloping hole into the surrounding soil. The single-chamber solution samplers used here and designed to be installed under a slight slope (15°), are constructed of porous stainless steel tubing 20.3 cm in length by 2.54 cm in diameter (outside) and extend from approximately 20 cm beyond the edge of the monitoring island walls (Young et al., 1999b). Dual-chamber solution samplers normally used for deep vertical installation (Soil Measurement Systems, Tucson, AZ) were installed in boreholes at a depth of 3 m at the locations shown by solid triangles in Fig. 1. The dual-chamber solution samplers are constructed of porous stainless steel tubing 9.5 cm in length by 5.0 cm in diameter (outside), welded to solid stainless steel tubing 30 cm in length and 5.0 cm in outside diameter and placed in a borehole. The dual-chamber solution samplers installed in the deep boreholes were completed using sieved native material (for details about the solution samplers and their installation see Young et al., 1999b).

Nine neutron probe access tubes were installed to a depth of 15 m deep (Fig. 1). Tensiometers were installed in a regular grid pattern across the plot at a depth of 3 m (nine locations, shown by solid triangles in Fig. 1, near the dual-chamber solution samplers), as well as at the monitoring islands (24 locations) from 0.5 m to a depth of 3.0 m in 0.5 m intervals.

Water with potassium bromide (KBr) was applied to the experimental plot using 164 drip lines. The parallel drip lines were spaced 0.3 m apart with self-cleaning emitters every 0.3 m along the line. A total of 27,000 emitters were so distributed over the 50 m × 50 m area.

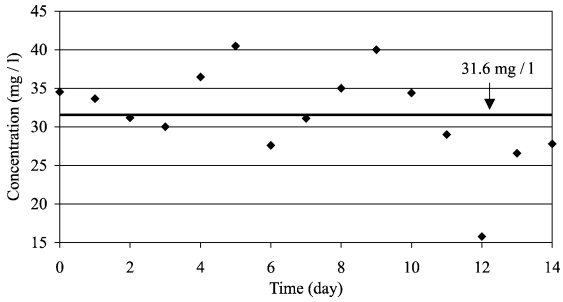

Fig. 2. Input concentrations of bromide during experiment I.

The experiment lasted 93 days, starting April 28, 1997 and ending on July 30, 1997. A KBr solution with a mean concentration of 31.6 ± 6.1 mg l^{-1} was applied for 15 days immediately followed by a 9-day application of irrigation water that contained less than 1.0 l^{-1} of bromide (April 28, 1997–May 21, 1997) at an average flux rate of 1.85 cm per day (cm d^{-1}) for an application of 44.4 cm of water and 2.19×10^7 mg of KBr. Redistribution of the solute in the profile was measured for 70 days following cessation of irrigation. The input concentration was quite variable due to problems with mixing of KBr in the supply tanks (Fig. 2). Young et al. (1999b) noted that it was difficult to control the fluid volume in the mixing tanks thereby creating a variable input bromide concentration during the irrigation period.

During the 93 days of the experiment, 898 samples were collected and analyzed for bromide from the monitoring island locations, 426 of these samples were collected during the irrigation period. At the deep borehole locations, 488 samples were collected and analyzed for bromide, 121 of these samples were collected during the irrigation period. Neutron probe data were collected in 0.25 m intervals from a depth of 0.25 m to the depth of the access tube (15 m). Tensiometer readings were collected for every 4 h at all installation locations.

2.3. Mass balance

The mass balance compares the amount of bromide in the water applied to the upper surface of the plot through the trickle system to the amount of bromide in the water contained within the soil profile at the monitoring island locations at specific times during

the experiment. The bromide mass present in the soil profile was determined by integrating the soil solution mass profile with depth for specific times during the experiment. The amount of bromide applied to the plot through the trickle system was calculated as a function of time as the average KBr input concentration multiplied by the volume of water measured from water meters located at the inlet water pipes of the irrigated plot. A mass balance was calculated according to the following equations:

$$\text{Mass balance} = M_{\text{measured}} - M_{\text{applied}} \quad (1)$$

$$M(z,t)_{\text{measured}} = \int_0^z \theta \Delta c \, \mathrm{d}z \quad (2)$$

$$\Delta c = c_{t=\text{time}} - c_{t=0} \quad (3)$$

where M is the mass of bromide (mg cm^{-2}), θ (cm^3 cm^{-3}) is the average water content in the profile, Δc (mg cm^{-3}) is the change in concentration from the initial condition, and z (cm) is the vertical depth interval represented by a given solution sampler (cm).

2.4. Effective flow and transport parameters

HYDRUS 1-D (Simunek et al., 1998) was utilized to simulate the flow of water and transport of bromide through the soil profile and to obtain transport parameters. The governing equations, without source or sink terms, are given by:

$$\frac{\partial \theta}{\partial t} = \frac{\partial}{\partial z}\left(K(h)\frac{\partial h}{\partial z}\right) + \frac{\partial K(h)}{\partial z} \quad (4)$$

$$\frac{\partial \theta R c}{\partial t} = \frac{\partial}{\partial z}\left(\theta D \frac{\partial c}{\partial z}\right) - \frac{\partial q c}{\partial z} \quad (5)$$

where θ is the volumetric water content (cm^3 cm^{-3}), t is time (day), K is hydraulic conductivity (cm d^{-1}), h is the water pressure head (cm), z is elevation increasing upwards (cm), R (dimensionless) is the retardation factor, c is the concentration (mg cm^{-3}), D is the dispersion coefficient (cm^2 d^{-1}), and q is the flux (cm d^{-1}).

Estimating the effective flow and transport parameters using the numerical model was a two-step process. During the first step, we used the average van Genuchten flow parameters θ_r, θ_s, α, and n (mean values of 0.078 cm^3 cm^{-3}, 0.35 cm^3 cm^{-3}, 0.0759 cm^{-1}, and 1.54, respectively) obtained by Fleming (2002) for 11 cores (7.5 cm OD by 7.5 cm long) taken 1.5 m below soil surface along a transect through the plot. No core hydraulic property data for depths other than 1.5 m are available. On the other hand, the hydraulic properties do vary with depth down to 3 m, and thus to take hydraulic property data from cores halfway down the profile is a reasonable first approximation. The K_s parameter was estimated by comparing simulated wetting front arrival times with observed arrival times as measured with tensiometers, and selecting the K_s value which resulted in the best fit between observed and simulated arrival times. The tensiometers responded very clearly and rapidly to the arrival of the wetting front and therefore, the tensiometer data provided the best data for signaling the arrival of the wetting fronts in the field. Problems in the tensiometer calibrations and the noise inherent in our field based neutron probe measurements made it difficult to use an inverse procedure such as in HYDRUS. The fitting process was repeated for 33 monitoring locations, 24 around the two monitoring islands, and nine at the 3 m depth, spread over the field site (Fig. 1). Note that for each of the 33 sites simulated, it was assumed that the soil profile above the site was uniform. Furthermore, the K_s values obtained are not true saturated conductivity values, but rather fitting parameters. No measured K_s values at depth are available and thus it is not known how the fitted K_s values compare to field measured values.

The transport parameters, D and R, were estimated in the second step. With the flow parameters known, we now optimized by trial and error values for D and R, again using HYDRUS in the forward mode. Most emphasis was placed on getting good fits between the front (rising) parts of the simulated and measured bromide breakthrough curves. For simplicity we used the average bromide input concentrations, rather than the actual values shown in Fig. 2. Simulations with either the actual or averaged bromide concentrations used for input showed very minimal differences in the parameter values obtained. Because the period during which water was applied lasted only 24 days, there was insufficient water applied for complete breakthroughs at all 3 m deep sites. In fact, at most sites the bromide concentrations increased, but never came down to near zero as they did at the shallower depths.

Effective transport properties were also estimated using an inverse analytical solution (Toride et al.,

1995) to the convective dispersion equation (Eq. (5)). This method differs from the trial and error numerical approach in that only the observed bromide concentrations collected during the irrigation time period, when the assumption of steady flow is assumed to be valid, were used for estimating the effective transport properties.

3. Results and discussion

3.1. Mass balance

A mass balance calculation was performed using Eqs. (1) and (2). Fig. 3 shows the bromide mass recovered from the soil profile at the two monitoring islands for 11 days during the time of bromide application. At the SMI (west side), the amount of bromide recovered was on average 112% of the amount applied; 97% of the applied mass was recovered on the east side. At the NMI, 90 and 119% was recovered from the east and west sides. At the four locations, the amounts of bromide recovered clearly increased with time, as expected. Although there is some variation, the amount of bromide recovered is close to the amount applied on all days. On average, 101% of the bromide was recovered, as shown by the mean recovery line shown (Fig. 3). Possible sources of error at the individual locations are anion exclusion, spatial variability in transport,

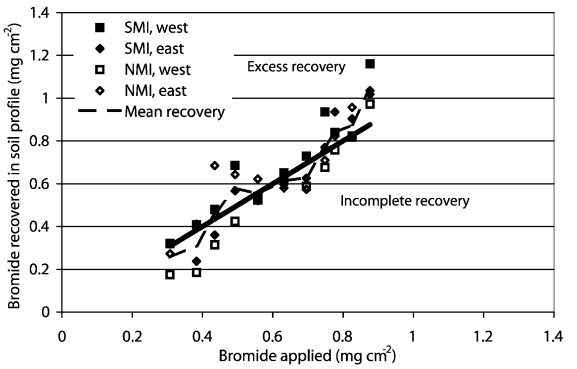

Fig. 3. Amounts of bromide recovered at the monitoring islands on days 5 through day 15 of the bromide application. The solid line represents 100% recovery. SMI and NMI are the north and south monitoring islands, respectively.

bias introduced by the measurement device (i.e. solution samplers), integration of the soil water profile, and analytical error in measuring the bromide concentrations.

Various investigators have found large variations in mass recovery of bromide using solution samplers. Ellsworth et al. (1996) found that solution samplers consistently under-estimated the applied mass for three tracers, bromide, nitrate, and chloride. The consistency between their breakthrough curves suggested that the poor mass recovery was not attributable to spatial variability or an inadequate number of measurements. Rather, the solution samplers measured the concentration only at the cup location and therefore did not provide a complete spectrum of the solute flow paths (Ellsworth et al., 1996). Adams and Gelhar (1992) found similar results when analyzing data from a 20-month natural gradient tracer study in the saturated zone of a highly heterogeneous aquifer. The solution samplers recovered 45–300% of the bromide mass. This large spread in mass recovery was attributed to spatial variability in the hydraulic conductivity and the sampling methodology, and reflected the effects of plume truncation, sampler bias, and possibly some type of tracer adsorption mechanism. Butters et al. (1989) refer to solution samplers as flux concentration detectors. They also measured some variation in the recovery of bromide mass using the samplers. The variation was attributed to variations in local flux rates, imprecision of solution samplers as flux concentration detectors, transient solute application rates and error introduced from sample extraction rates that are higher or lower than the drainage flux which can cause an over- or under-estimation of the bromide mass (Butters et al., 1989). Roth et al. (1991) used data from a chloride tracer test that was monitored using solution samplers to quantify preferential flow. Using predictions from a fitted convection–dispersion model, they found that due to preferential flow the main pulse contained less than half of the applied solute mass while the remaining mass was contained in several smaller solute pulses of varying velocities that split from the main solute pulse.

Anion exclusion can also contribute to the bromide mass balance error. Anion exclusion can cause bromide to be mostly located near the centers of

the pore channels. The pore water extracted using solution samplers is from the entire pore channel (excluding of course, the adhesive water around the soil grain), which includes the water from the sides of the pore channels that contain no anions, an excluded volume. Pore water extracted from the excluded volume added to the volume containing the bromide anion results in a diluted measured concentration of bromide. In addition, anions traveling near the center of the pores may travel faster than the average pore-water velocity, causing some of the bromide to travel further than the lowest solution samplers at the monitoring islands during the sampling time interval resulting in a truncation of the solute concentration profile. Local average pore-water velocities that are greater than the calculated values could further enhance this effect.

In view of all these uncertainties, our mass balances of 112, 97, 90, and 119% at the four monitoring island locations are in fact quite acceptable.

Table 1
Fitted hydraulic conductivity (K_s) parameter values for monitoring island locations

Depth (cm)	K_s (cm d^{-1})
SMI-West	
50	15
100	25
150	35
200	70
250	75
300	100
SMI-East	
50	15
100	25
150	40
200	72
250	75
300	100
NMI-West	
50	15
100	50
150	125
200	125
250	175
300	190
NMI-East	
50	40
100	76
150	75
200	92
250	100
300	165
Mean	78.1
Standard deviation	50.5
CV (%)	64.7

3.2. Effective flow and transport parameters

3.2.1. Flow parameters

Tables 1 and 2 contain the fitted hydraulic conductivity (K_s) parameter values for the monitoring islands and nine field locations, respectively. These parameter values were obtained by fitting predicted water front arrivals (and water content distributions) to measured values using the same laboratory determined values for θ_r, θ_s, α, and n for all 33 locations. An example of measured versus fitted water contents is presented in Fig. 4 for the 150 cm depth at the four monitoring island locations. The variations in tension recorded with pressure transducers connected to a datalogger are also presented. We deleted the vertical tension scale, because the transducer calibration data were incomplete. Nevertheless these tension data clearly show the arrivals of the wetting fronts, and also the beginning of drainage upon termination of water application. The magnitude of the tension data was between 40 and 300 cm, with

Table 2
Fitted hydraulic conductivity (K_s) parameter values for the nine field locations at 300 cm

NP#/SS#	K_s (cm d^{-1})
300 cm depth	
402/303	135
403/313	190
415/323	120
422/333	200
423/343	135
424/353	135
442/363	165
443/373	165
445/383	95
Mean	149
Standard deviation	33.8
CV (%)	22.7

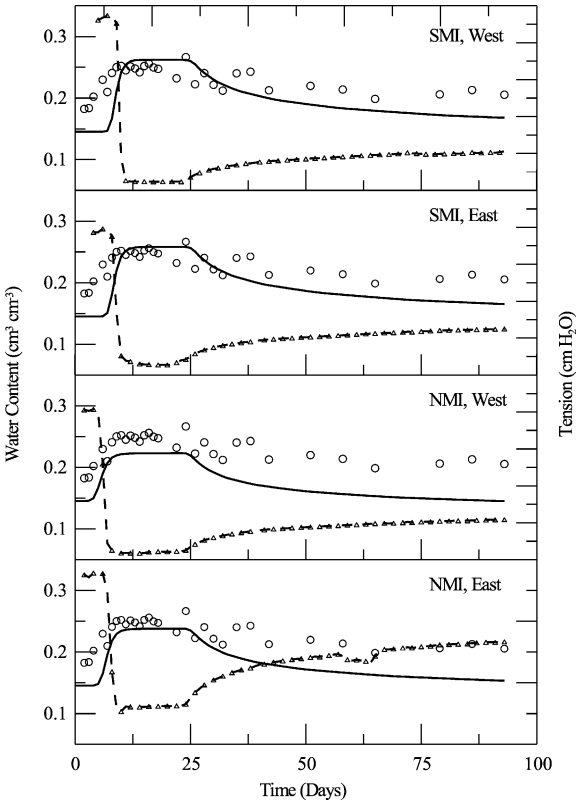

Fig. 4. Variation in water content and tension (dashed line) with time at the four monitoring island locations at the 150 cm depth. Open circles are measured water contents. Solid lines represent simulated water contents. Note the vertical tension scale is missing because of insufficient data for the pressure transducers used in each tensiometer. On average, the tension reached about 100 cm on day 75.

the average tension approaching 100 cm around day 75. It was found during the simulations that K_s needed to be changed with depth to obtain agreement between observed and predicted water front arrival times. Thus at this site we needed to increase K_s from about 21 cm d^{-1} at the 50 cm depth, to on average 146 cm d^{-1} at the 300 cm depth. This increase in saturated conductivity is related to increases in sand and gravel with depth between the surface and the 300 cm depth (Thomasson, 2000).

3.2.2. Transport parameters

Tables 3 and 4 contain the fitted effective transport parameters, for the monitoring island and nine field locations, respectively. These tables show the values of the dispersion coefficients and retardation factors that produce close agreement between measured and modeled bromide versus time distributions (Figs. 5–7). The mean dispersion coefficient for all monitoring island locations and depths is 3.55 cm^2 d^{-1}, with a coefficient of variation of 81%. For the nine field locations at 3 m, it is 5.28 cm^2 d^{-1} with a coefficient of variation of 30%. Assuming an

Table 3
Numerically fitted transport properties for the monitoring island locations

Location/depth (cm)	D (cm^2 d^{-1})	R
SMI-W/50	1.10	0.52
SMI-E/50	4.50	0.75
NMI-W/50	8.50	0.78
NMI-E/50	1.50	0.51
Mean	3.90	0.64
SMI-W/100	3.25	0.58
SMI-E/100	2.25	0.82
NMI-W/100	2.00	0.99
NMI-E/100	1.75	0.86
Mean	2.31	0.81
SMI-W/150	4.25	0.72
SMI-E/150	1.50	1.00
NMI-W/150	2.25	1.10
NMI-E/150	1.10	0.95
Mean	2.28	0.94
SMI-W/200	3.75	0.65
SMI-E/200	3.50	1.04
NMI-W/200	1.75	1.17
NMI-E/200	1.10	0.85
Mean	2.53	0.93
SMI-W/250	3.50	0.53
SMI-E/250	3.75	0.94
NMI-W/250	9.25	1.15
NMI-E/250	2.50	0.83
Mean	4.75	0.86
SMI-W/300	1.00	0.52
SMI-E/300	5.50	0.80
NMI-W/300	12.50	1.02
NMI-E/300	3.10	0.76
Mean	5.53	0.77
For all depths		
Mean	3.55	0.83
Standard deviation	2.87	0.20
CV (%)	80.79	24.61

Table 4
Numerically fitted transport properties for the nine field locations at 300 cm

NP#/SS#	D (cm^2 d^{-1})	R
402/303	5.00	0.45
403/313	5.00	0.50
415/323	4.50	0.57
422/333	3.75	0.56
423/343	6.00	0.57
424/353	5.00	0.50
442/363	6.00	0.55
443/373	3.50	0.49
445/383	8.75	0.87
Mean	5.28	0.56
Standard deviation	1.56	0.12
CV (%)	29.53	21.78

average field water content from neutron probe data of 0.22 cm^3 cm^{-3}, and a flux of 1.85 cm d^{-1}, we get a mean pore-water velocity of 8.4 cm d^{-1}. This results in mean dispersivity values of 0.64 cm for the lysimeter sites and 1.5 cm for the field sites. These relatively low dispersivity values are of the same order of magnitude and are in agreement with dispersivity values we obtained at other controlled, unsaturated field transport studies (Wierenga et al., 1990).

The retardation factors calculated for the monitoring island and the nine field locations range from 0.45 to 1.17, with 27 of the 33 values being less than 1. For the nine field locations, R values range between 0.45 and 0.87, and the coefficient of variation is 22%. The bromide distribution curves at the monitoring island

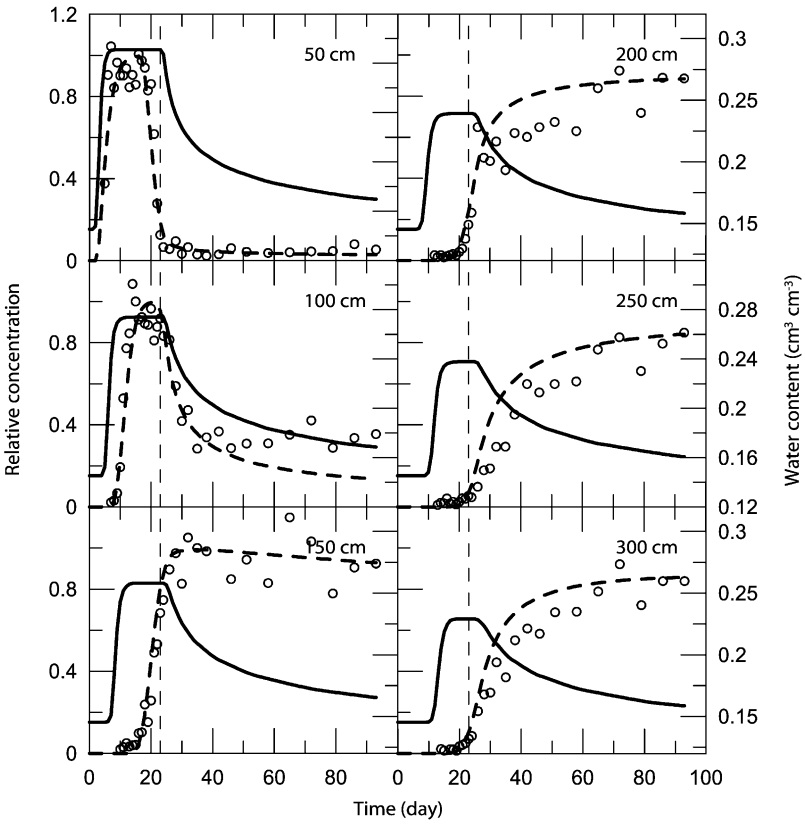

Fig. 5. Comparison of measured bromide data (circles) and the fitted bromide concentrations (dashed lines) at the SMI, east location. The solid line represents model predictions for water content changes. The vertical dashed line signals the end of water application.

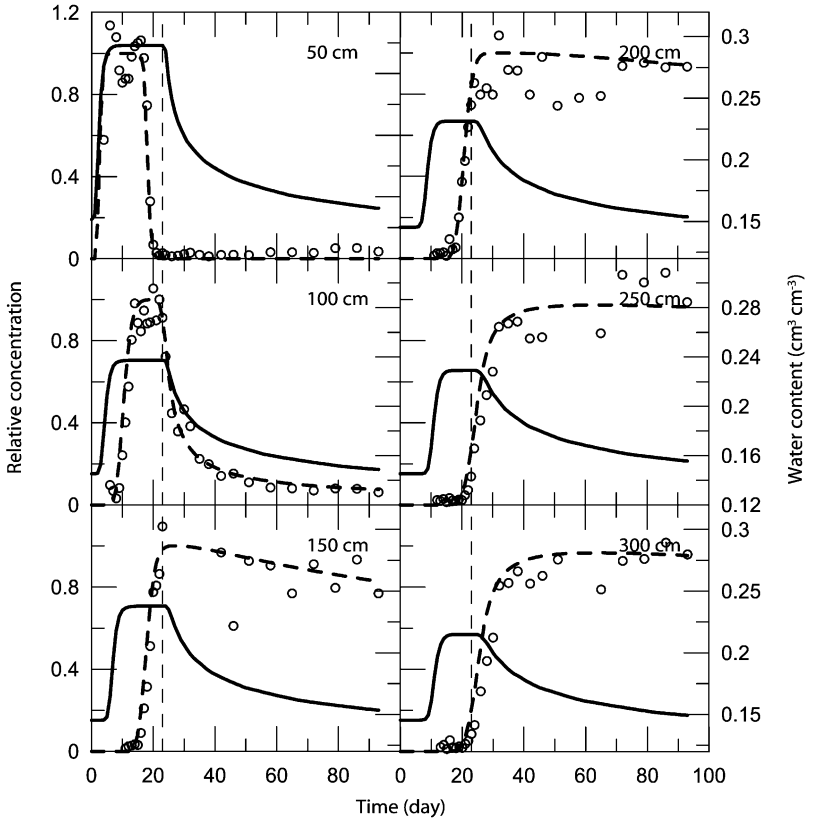

Fig. 6. Comparison of measured bromide data (circles) and the fitted bromide concentrations (dashed lines) at the NMI, east location. The solid line represents model predictions for water content changes. The vertical dashed line signals the end of water application.

locations are well described with the 1-D numerical model with a bulk transport coefficient or retardation factor that is mostly less than one (Figs. 5 and 6). The fit is also good for the breakthrough portion of the bromide distribution curves at the nine field locations (Fig. 7), but less good for the tail ends of these curves. Thus it appears that for the monitoring island sites, the use of a conceptual model with only one transport parameter for describing the arrival of the bromide is acceptable, but not for the field sites. For the nine field locations a multi-parameter transport model, such as the mobile immobile model (van Genuchten and Wierenga, 1976), might be expected to better describe the tail ends of the bromide distribution curves. The reasons for the differences in the goodness of fit between the bromide distributions at 3 m at the monitoring island sites versus the nine field locations are not known. For the nine field locations, the solution samplers were separated horizontally up to 3 m (approximately 12 m at two locations) from the neutron probes. This could have caused differences between the water contents at the lysimeters and at the neutron probe access tube locations. Errors in the field water content could also have resulted from using an incorrect calibration curve for computing water contents from neutron count rates. This would have affected all water contents and in as much as the tail ends of nearly all the field bromide concentration distributions are not well predicted, it is possible that errors in water content measurements are the main cause for the large differences between measured and predicted tail end bromide concentrations. For the bromide distribution predictions at the monitoring islands, water content data from one neutron probe access tube located between the two monitoring islands was used. The total water held in the profile

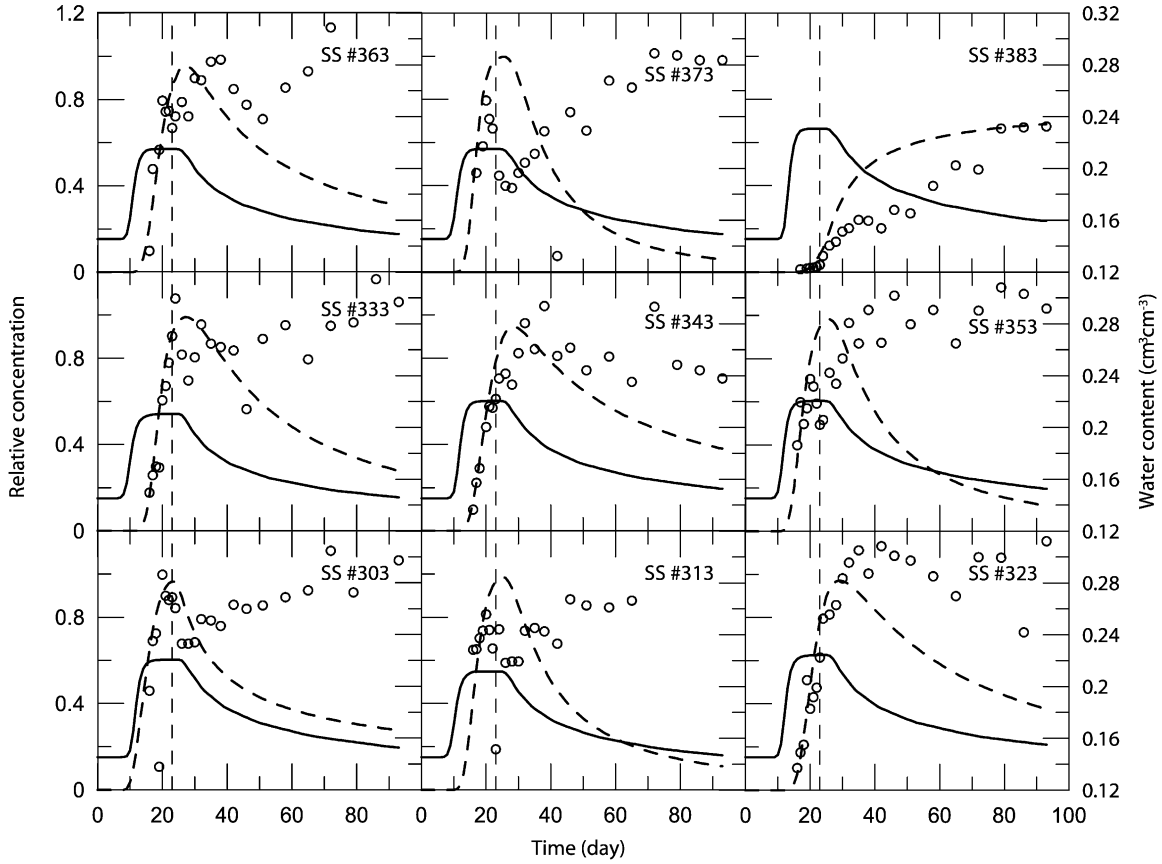

Fig. 7. Comparison of measured bromide data (circles) and the fitted bromide concentrations (dashed lines) at the nine field locations at the 3 m depth. The vertical dashed line signals the end of water application.

at this neutron probe site apparently was the correct one to use, because even after 24 days of irrigation (15 days with bromide, followed by 9 days with no bromide water) the observed as well as the modeled bromide at 1.5 m and below did not decrease in concentration.

The data in Figs. 5–7 clearly show that the solute front in this unsaturated flow and transport experiment stays behind the wetting front. This is as expected (Warrick et al., 1971; De Smedt and Wierenga, 1978; Ghuman and Prihar, 1980) and is a result of the presence of bromide free water in the soil before the start of water application. Because the soil was initially drier near the surface, the delay in arrival of bromide at 50 cm is less as compared to the arrival of the bromide at deeper depths (Figs. 5 and 6). As the initial water content in the soil increases with depth, the time lag increases (Table 5).

Although the experiment described is a transient experiment, the facts that the solute fronts lag behind the wetting fronts and that the application rate is constant make it feasible to use an analytical solution to estimate the transport parameters. The results of this analysis for the monitoring island locations are presented in Table 6. The data in this table show good agreement, on average, with the results in Table 3. Although the mean dispersion coefficient is somewhat larger if estimated with the analytical solution, the mean retardation factors are nearly identical (0.78 versus 0.83 in Table 3). This gives further confidence in the retardation factors estimated with the numerical procedure.

Table 5
Arrival times for the wetting front and bromide and the lag times

Location	Depth (cm)	WF arrival (day)	Br arrival (day)	Lag (day)
201	50	4.0	3.1	−0.9
211	50	4.0	5.3	1.3
241	50	4.0	6.5	2.5
251	50	3.0	3.9	0.9
Mean		3.8	4.7	0.9
202	100	7.5	9.0	1.5
212	100	6.5	10.9	4.4
242	100	5.5	12.5	7.0
252	100	4.5	11.5	7.0
Mean		6.0	11.0	5.0
203	150	9.5	15.0	5.5
213	150	9.0	21.0	12.0
243	150	6.0	19.4	13.4
253	150	7.5	19.0	11.5
Mean		8.0	18.6	10.6
204	200	11.0	15.2	4.2
214	200	11.5	25.3	13.8
244	200	8.0	37.3	29.3
254	200	9.0	21.0	12.0
Mean		9.9	24.7	14.8
205	250	13.0	18.0	5.0
215	250	13.0	39.3	26.3
245	250	10.0	24.3	14.3
255	250	11.5	27.5	16.0
Mean		11.9	27.3	15.4
206	300	14.0	19.8	5.8
216	300	14.0	37.0	23.0
246	300	11.0	25.5	14.5
256	300	12.0	29.3	17.3
Mean		12.8	27.9	15.2
For all depths				
Mean		8.7	19.0	10.3
Standard deviation		3.3	10.4	7.6
CV (%)		38.4	54.8	73.6

Table 6
Analytically estimated transport properties for the monitoring island locations

Location/depth (cm)	D (cm^2 d^{-1})	R
SMI-W/50	4.74	0.50
SMI-E/50	10.96	0.79
NMI-W/50	8.34	1.03
NMI-E/50	7.14	0.51
SMI-W/100	3.03	0.66
SMI-E/100	5.77	0.81
NMI-W/100	18.13	0.94
NMI-E/100	14.07	0.84
SMI-W/150	2.06	0.76
SMI-E/150	19.02	1.11
NMI-W/150	18.03	1.00
NMI-E/150	7.09	0.96
SMI-W/200	3.90	0.61
SMI-E/200	N/A	N/A
NMI-W/200	N/A	N/A
NMI-E/200	12.83	0.84
SMI-W/250	3.65	0.61
SMI-E/250	N/A	N/A
NMI-W/250	N/A	N/A
NMI-E/250	N/A	N/A
SMI-W/300	3.54	0.56
SMI-E/300	N/A	N/A
NMI-W/300	N/A	N/A
NMI-E/300	N/A	N/A
Mean	8.89	0.78
Standard deviation	5.85	0.19
CV (%)	65.80	24.63

4. Conclusions

The results show that for the MAC site water infiltration into unsaturated soil could be predicted with a 1-D numerical model using van Genuchten parameters (θ_r, θ_s, α, and n) obtained from undisturbed cores collected from the 1.5 m depth. However, we found that the saturated conductivity value K_s obtained from cores was not applicable to the field data. We had to use a K_s value that increased with depth due to increasing amounts of gravel and sand with depth. Bromide breakthrough curves were well simulated down to 3 m with a 1-D transport equation, and with fitted bulk retardation factors which ranged from 0.45 to 1.02 at the 3 m depth. The average dispersion coefficient for the 13 measurement sites at 3 m was 5.35 cm^2 d^{-1} with a CV of 52%. The average retardation factor at 3 m was 0.63. The coefficient of variation for the retardation factor for the 13 measurement sites at 3 m in this 50 m × 50 m plot is 28%.

We found that with an average R value of 0.63, but ranging from 0.45 to 1.17, there was good agreement between measured and predicted

bromide arrival times. However, note that this fairly wide range in R values was obtained after optimizing the hydraulic parameters to the flow data at each site. The solution samplers by necessity were horizontally separated from the neutron probe and tensiometers by at least 2 m, and this can explain some of the variability in R values. However, after first optimizing the flow data, one would have expected a narrower range in R values for this $50\,m \times 50\,m$ site. Nevertheless, for many practical situations one is mostly interested in first arrival of a contaminant, and it is for this reason that a simplified approach as used here may be useful. However, our data suggest that when using such a simple field approach, and in order to not under-estimate the solute arrival times one should use a range of R values, not unlike what we found in this study. Additional studies are underway to see if the modeling results for the 3 m depths apply to the 5 and 10 m depths at this site.

Acknowledgements

The authors acknowledge the support of the U.S. Nuclear Regulatory Commission, Washington, D.C., under contract NRC-04-97-056. Thomas J. Nicholson, Project Manager.

References

Adams, E.E., Gelhar, L.W., 1992. Field study of dispersion in a heterogeneous aquifer. 2. Spatial moments analysis. Water Resources Research 28 (12), 3293–3307.

Arizona Department of Water Resources, 1993. Arizona Water Resources Assessment, Hydrologic Summary, vol. 2., p. 243.

Beven, K., Germann, P., 1982. Macropores and water flow in soils. Water Resources Research 18 (5), 1311–1325.

Biggar, J.W., Nielsen, D.R., 1976. Spatial variability of the leaching characteristics of a field soil. Water Resources Research 12 (1), 78–84.

Brusseau, M.L., 1994. Transport of reactive contaminants in heterogeneous porous media. Reviews of Geophysics 32 (3), 285–313.

Butters, G.L., Jury, W.A., Ernst, F.F., 1989. Field scale transport of bromide in an unsaturated soil. 1. Experimental methodology and results. Water Resources Research 25 (7), 1575–1581.

Dagan, G., Bresler, E., 1979. Solute Dispersion in Unsaturated Heterogeneous Soil at Field Scale: I. Theory. Soil Science Society of America Journal 43 (3), 461–467.

De Smedt, F., Wierenga, P.J., 1978. Approximate analytical solution for solute flow during infiltration and redistribution. Soil Science Society of America Journal 42 (3), 407–412.

Ellsworth, T.R., Shouse, P.J., Skaggs, T.H., Jobes, J.A., Fargerlund, J., 1996. Solute transport in unsaturated soil: experimental design, parameter estimation, and model discrimination. Soil Science Society of America Journal 60 (2), 397–407.

Fleming, J.B., 2002. Applications of the inverse approach for estimating unsaturated hydraulic parameters from laboratory outflow experiments. PhD thesis, The University of Arizona.

van Genuchten, M.T., Wierenga, P.J., 1976. Mass transfer studies in sorbing porous media I. Analytical solutions. Soil Science Society of America Journal 40 (4), 473–480.

Ghuman, B.S., Prihar, S.S., 1980. Chloride displacement by water in homogeneous columns of three soils. Soil Science Society of America Journal 44 (1), 17–21.

James, R.V., Rubin, J., 1986. Transport of chloride ion in a water-unsaturated soil exhibiting anion exclusion. Soil Science Society of America Journal 50 (5), 1142–1149.

Jury, W.A., Stolzy, L.H., Shouse, P., 1982. A field test of the transfer function model for predicting solute transport. Water Resources Research 18 (2), 369–375.

Jury, W.A., Sposito, G., White, R.E., 1986. Transfer function model of solute transport through soil: 1. Fundamental concepts. Water Resources Research 22 (2), 243–247.

Porro, I., Wierenga, P.J., 1993. Transient and steady-state solute transport through a large unsaturated soil column. Ground Water 31 (2), 193–200.

Roth, K., Jury, W.A., Flühler, H., Attinger, W., 1991. Transport of chloride through an unsaturated field soil. Water Resources Research 27 (10), 2533–2541.

Russo, D., 1998. Stochastic analysis of flow and transport in unsaturated heterogeneous porous formation: effects of variability in water saturation. Water Resources Research 34 (4), 569–581.

Russo, D., Bresler, E., 1981. Soil hydraulic properties as stochastic processes: I. An analysis of field spatial variability. Soil Science Society of America Journal 45 (4), 682–687.

Simunek, J., Sejna, M., van Genuchten, M.T., 1998. The HYDRUS-1D software package for simulating the one-dimensional movement of water, heat, and multiple solutes in variably saturated media. Version 2.0. U.S. Salinity Laboratory, USDA, ARS, Riverside, CA, p. 178.

Simunek, J., Jarvis, N.J., van Genuchten, M.T., Gärdenäs, A., 2003. Nonequilibrium and preferential flow and transport in the vadose zone: review and case study. Journal of Hydrology, This issue.

Thomasson, M.J., 2000. Hysteretic, variably saturated, transient flow and transport models with numerical inversion techniques to characterize a field soil in central Arizona. PhD thesis, The University of Arizona.

Toride, N., Leij, F.J., van Genuchten, M.Th., 1995. The CXTFIT code estimating transport parameters from laboratory or field

tracer experiments. Version 2.0. U.S. Salinity Laboratory, USDA, ARS, Riverside, CA, p. 121.

Warrick, A.W., Biggar, J.W., Nielsen, D.R., 1971. Simultaneous solute and water transfer for an unsaturated soil. Water Resources Research 7 (5), 1216–1225.

Wierenga, J., Hudson, D.B., Hills, R.G., Porro, I., Vinson, J., Kirkland, M.R., 1990. Flow and Transport Experiments at the Las Cruces Trench Site: Experiments 1 and 2, U.S. Nuclear Regulatory Commission Report,.

Young, M.H., Wierenga, P.J., Warrick, A.W., Hofmann, L.L., Musil, S.A., 1999a. Variability of wetting front velocities during a field-scale infiltration experiment. Water Resources Research 35 (10), 3079–3087.

Young, M.H., Wierenga, P.J., Warrick, A.W., Hofmann, L.L., Musil, S.A., Yao, M., Mai, C.J., Zou, Z., Scanlon, B.R., 1999b. Results of field studies at the Maricopa Environmental Monitoring Site, Arizona, U.S. Nuclear Regulatory Commission, Washington, D.C., p. 260.